Quantum Molecular Dynamics Study of the Reaction of O_2 with HOCO†

Hua-Gen Yu* and James T. Muckerman

Department of Chemistry, Brookhaven National Laboratory, Upton, New York 11973-5000

Received: October 3, 2005; In Final Form: November 7, 2005

The reaction of O_2 with HOCO has been studied by using an ab initio direct dynamics method based on the UB3PW91 density functional theory. Results show that the reaction can occur via two mechanisms: direct hydrogen abstraction and an addition reaction through a short-lived $HOC(O)O_2$ intermediate. The lifetime of the intermediate is predicted to be 660 ± 30 fs. Although it is an activated reaction, the activation energy is only 0.71 kcal/mol. At room temperature, the obtained thermal rate coefficient is 2.1×10^{-12} cm^3 molecule^{-1} s^{-1}, which is in good agreement with the experimental results.

1. Introduction

The reaction of the hydroxyl radical with carbon monoxide, $OH + CO \rightarrow H + CO_2$, is the major process by which CO is removed by oxidation in combustion and atmospheric environments.[1,2] There are many experimental[3−15] and theoretical[16−36] studies on its kinetics and dynamics. The reaction occurs via a long-lived HOCO complex due to the existence of a deep well along the reaction pathway. Accurate ab initio calculations[26,28] show that the potential well for HOCO is as deep as 30.10 kcal/mol with respect to the OH + CO reactants. Since the dissociation barrier of HOCO to the $H + CO_2$ products is also very high, the HOCO intermediate can be significantly stabilized by a third collision partner in a realistic reaction system. The HOCO radical was first comfirmed by Milligan and Jacox[37] in a matrix spectroscopy study. Now, the structures[26,28,38,39] and energetics of both *cis*- and *trans*-HOCO comformers are well-established.

Pressure-dependent experimental studies[40−44] have indicated that there is an appreciable abundance of stabilized HOCO in combustion and atmospheric environments, and it becomes important to study the reactivity of the HOCO radical with other radicals or molecules. Recently, a few reactions, including the reactions of HOCO with NO, O_2, and OH, have been reported.[41,45−49] In particular, the $O_2 + HOCO \rightarrow HO_2 + CO_2$ reaction is of the most importance in atmospheric and combustion processes, since the O_2 reactant has a large abundance. The HO_2 product is also a crucial species in chain reactions. Most recently, the reaction pathways were investigated by Poggi and Francisco[48] using a high-level ab initio method. Their calculations suggested that both direct abstraction and addition mechanisms could coexist for this reaction. It is an activated reaction with small transition-state barriers in the entrance channels.

However, kinetics and dynamics studies of the $O_2 + HOCO$ reaction are scarce. To our best knowledge, only the thermal rate coefficient at room temperature has been measured.[41,46,47] The rate coefficient has been determined to be $1.44-1.9 \times 10^{-12}$ cm^3 molecule^{-1} s^{-1}, which is smaller by a factor of 5.5 than that calculated for the OH + HOCO reaction.[49] The temperature dependence of the thermal rate coefficient is unknown.

In this work, we have carried out an ab initio direct dynamics study for this reaction. Here, the reaction mechanism and the lifetime of the $HOC(O)O_2$ intermediate complex are addressed. Besides the detailed dynamics studies, the thermal rate coefficients of the $O_2 + HOCO \rightarrow HO_2 + CO_2$ reaction are calculated in the temperature range from 200 K to 1000 K.

2. Dynamics Method

The *DualOrthGT* program[50] was used in the dynamics calculations. Trajectories were propagated with a time step of 0.48 fs for a set of randomly sampled initial conditions, where only the collision energy was held at a fixed value. The orientation, rotational energy, and vibrational phases of reactants were selected according to the canonical ensemble at $T = 300$ K. The initial center-of-mass distance between the O_2 and HOCO reactants was set as $\rho_0 = \sqrt{R_0^2+b^2}$ with $R_0 = 12.5\ a_0$, where $b = \zeta^{1/2} b_{max}$ is the impact parameter. Here, ζ is a uniformly distributed random number in (0, 1), and b_{max} is the maximum impact parameter. All trajectories were terminated when the separation distance between any two fragments of the system is larger than $9.0\ a_0$ once the reactants had collided.

The forces used in trajectory propagations are determined "on the fly" by a hybrid DFT method,[51] UB3PW91/6-31G(d). This ab initio method was selected by minimizing the errors of the relative energies of the stationary points on the ground-state electronic surface of $HOC(O)O_2$ with respect to the best ab initio values of Poggi and Francisco.[48] A comparison of the calculated energies for the $O_2 + HOCO \rightarrow HO_2 + CO_2$ reaction is given in Table 1. As labeled in ref 48, TSa refers to the transition state for the O_2 addition to HOCO to form a $HOC(O)O_2$ intermediate, whereas TSb stands for its dissociation barrier to the $HO_2 + CO_2$ products. TSc is the transition state for the direct H-abstraction reaction from the reactants to the products. Table 1 shows that the overall agreement is good. The mean average errors are 1.9 kcal/mol. In particular, the barrier height for the key transition state TSa is obtained as 1.15 kcal/mol, which is comparable to the best value of 1.6 kcal/mol. In general, the DFT method has slightly underestimated the barrier height, but the major profile of the potential energy surface should be acceptable in the dynamics studies for this reaction. In this work, all electronic structure calculations were carried out using the *Gaussian 03* program.[51]

† Part of the special issue "John C. Light Festschrift".

* E-mail: hgy@bnl.gov. Fax:+1-631-344 5815.

10.1021/jp055623j CCC: $33.50
Published on Web 12/10/2005

TABLE 1: Relative Energies and Zero-Point Energies (ZPE)[a]

species	ΔE	ZPE	ΔH(0 K)	ΔH(0 K)[b]
O_2 + HOCO	0.0	15.33	0.0	0.0
HO_2 + CO_2	−43.78	15.90	−43.21	−46.8
(trans,trans)-HOC(O)O_2	−38.94	18.57	−35.70	−38.2
TSa	+0.72	15.76	+1.15	+1.6
TSb	−32.16	16.01	−31.48	−33.4
TSc	+1.08	14.83	+0.58	+3.5

[a] Values in kcal/mol and calculated with the UB3PW91/6-31G(d) method, where the ZPEs are scaled by a factor[57] of 0.9772, and the energy zero is set at the reactant asymptote. The UB3PW91 energy is −339.27869 au at the O_2 + HOCO limit. [b] The QCISD(T)/6-311++G(3df,3pd) energies taken from ref 48.

Reaction cross-sections at a collision energy of E_T are calculated as[52,53]

$$\sigma_r(E_T) = \pi b_{max}^2 P_r \quad (1)$$

with the reaction probability

$$P_r = N_r/N \quad (2)$$

where N_r is the number of reactive trajectories of a total of N trajectories. The cross-section error is given by

$$\Delta\sigma_r = \left[\frac{N - N_r}{NN_r}\right]^{1/2} \sigma_r \quad (3)$$

From the total reactive cross-sections, and assuming a Maxwell−Boltzman distribution over the translational energy, the thermal rate coefficients are determined by

$$k(T) = g_e\left(\frac{8}{\pi\mu(k_BT)^3}\right)^{1/2} \int_0^\infty E_T\sigma_r(E_T)\, e^{-E_T/k_BT}\, dE_T \quad (4)$$

where $g_e = {}^1/_3$ is the electronic statistical factor for the reaction occurring on the ground electronic state, and μ is the reduced mass of the reactants. Other symbols have their usual meanings.

During the simulated collisions, the molecular fragments and shape of the collision system are identified using graph theory as in our previous work.[54] Similarly, we used a numerical tag to trace the HOC(O)O_2 complex so that its lifetime (τ) can be extracted for each trajectory. Here, the chemical bond criteria (see eq 9 in ref 54) for the formation of the complex are α_{OO} = 3.6 a_0, α_{CO} = 3.9 a_0, α_{OH} = 2.8 a_0, and α_{CH} = 3.0 a_0. Finally, the lifetime of the complex is calculated according to its survival probability, $P_S(t)$, where the time zero ($t = 0$) is defined by the first formation of the HOC(O)O_2 molecule in each trajectory, as

$$P_S(t) = e^{-t/\tau} \quad (5)$$

3. Results and Discussion

We have carried out a total of 2228 trajectories at 5 given collision energies. In the calculations, the maximum impact parameter is set to be b_{max} = 5.5 a_0. This is a somewhat small value for a radical−radical reaction, but consistent with the character of the potential energy surface with a low barrier along the reaction pathway. The dynamics results are summaried in Table 2. Actually, 500 trajectories were run for each given energy, but we discarded some trajectories that started in an electronically excited state of the HOCO radical. For the collision energies of interest, only the HO_2 + CO_2 product channel is open.

TABLE 2: Dynamics Results for the O_2 + HOCO Reaction[a]

E_T/kcal·mol^{-1}	N	$N_r(N_d/N_C)$	P_r	σ_r/a_0^2	$\Delta\sigma_r/a_0^2$
0.5	448	12(6/6)	0.02678	2.545	0.720
1.0	463	17(7/10)	0.03672	3.489	0.830
2.5	448	32(2/30)	0.07143	6.788	1.156
5.0	442	40(2/38)	0.09050	8.600	1.297
8.0	427	45(2/43)	0.10539	10.015	1.412

[a] N_d and N_C are the number of direct abstraction and short-lived complex reactive trajectories, respectively.

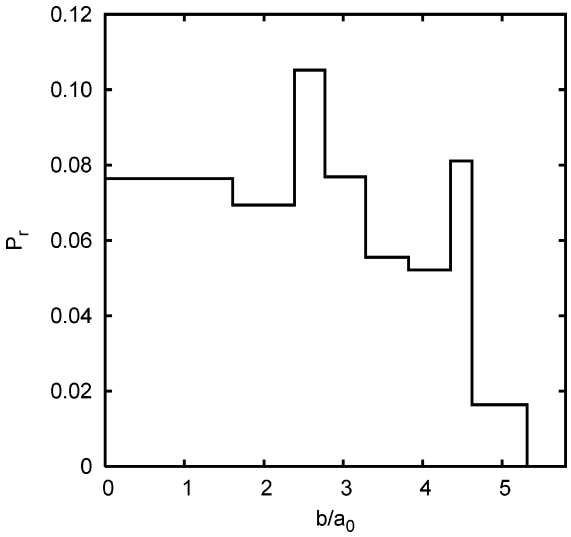

Figure 1. Opacity function for the total reaction probability of the O_2 + HOCO reaction calculated with all 2228 trajectories.

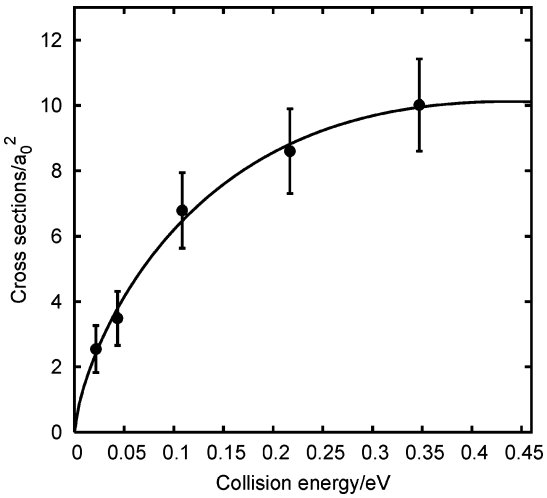

Figure 2. Reactive cross-sections for the O_2 + HOCO reaction, where the points with error bars are the calculated results together with the fitting curve as a solid line.

Figure 1 shows the opacity function for the O_2 + HOCO reaction. Since the maximum impact parameters are not very sensitive to the small range of collision energies, we have combined data from all the collision energies in plotting this figure in order to get a better statistical profile. The figure clearly shows that the reaction probability is small, which implies that it is a slow reaction.

Reactive cross-sections for the O_2 + HOCO → HO_2 + CO_2 are displayed in Figure 2; also indicated are the calculated 68% error bars. The results show that there is no significant threshold energy for reaction, although it is an activated reaction. This is

TABLE 3: Calculated Thermal Rate Coefficients $k(T)$ (cm^3 $molecule^{-1}$ s^{-1}) for the O_2 + HOCO Reaction Together with the Experimental Results

T/K	$10^{12} \times k(T)$	expt[41,46,47]
200	1.36	
250	1.74	
298	2.11	1.9 ± 0.2[46]
		1.64 ± 0.25[47]
		1.44 ± 0.3[41]
350	2.51	
400	2.90	
500	3.65	
600	4.39	
800	5.79	
1000	7.08	

because the quasi-classical trajectories (QCT) can leak some vibrational energy of the reactants into the relative translational energy, which can lead trajectories to overcome the small transition barriers in the entrance channel. As a result, the QCT method will overestimate the reaction probability. On the other hand, however, the missing treatment of quantum tunneling effects for this hydrogen transfer reaction will underestimate the reaction probability. In practice, these factors tend to compensate each other well. As discussed by Guo et al.,[55] the final QCT results are usually accurate, especially for statistically averaged quantities. Moreover, the reaction cross-sections can be fitted well using form

$$\sigma_r(E_T) = CE_T^n e^{-mE_T} \tag{6}$$

where C, n, and m are least-squares fitting parameters. Their optimal values are $C = 36.114 \pm 11.38$, $n = 0.696\,612 \pm 0.1029$, and $m = 1.591\,18 \pm 0.6485$ in units of eV and a_0. The fitted curve is also shown in Figure 2.

By placing eq 6 in eq 4, one can obtain the following analytical expression for the rate coefficients:[56]

$$k(T) = C\left(\frac{8k_BT}{\pi\mu}\right)^{1/2}\frac{\Gamma(n+2)(k_BT)^n}{(1+mk_BT)^{n+2}} \tag{7}$$

For the temperature range 200−1000 K, the calculated thermal rate coefficients for the O_2 + HOCO reaction are given in Table 3 together with the experimental results for comparison. The rate coefficient at room temperature is obtained as 2.1×10^{-1} cm^3 $molecule^{-1}$ s^{-1}. It is in good agreement with the observed values[41,46,47] of $1.44-1.9 \times 10^{-12}$ cm^3 $molecule^{-1}$ s^{-1}. Obviously, the reaction is slow for a radical−radical reaction.

Furthermore, the temperature dependence of the rate coefficient is weak. At low and medium temperatures, the denominator $(1 + mk_BT)^{n+2}$ in eq 7 is not strongly dependent on T. As a result, the temperature dependence of the thermal rate coefficient is approximately $T^{n+0.5}$, which is close to a linear dependence with $n = 0.697$. According to such a dependence, the activation energy can be estimated as $E_a \approx (n + 0.5)k_BT$. At room temperature, the activation energy is about 0.71 kcal/mol.

By taking advantage of the molecular dynamics method, one can study reaction mechanisms in detail. It was found that there exist two mechanisms: direct abstraction and an addition reaction via a short-lived complex. The addition mechanism[41] has been well-established experimentally. Most recently, the ab initio calculations of Poggi and Francisco[48] also suggested that the reaction could occur via a direct H-abstraction mechanism. Their prediction is substantiated by the present dynamics study. Two typical direct abstraction trajectories are illustrated in Figure 3. Both trajectories have the same collision energy of 0.5 kcal/mol and intial rotational and vibrational energy, but the impact

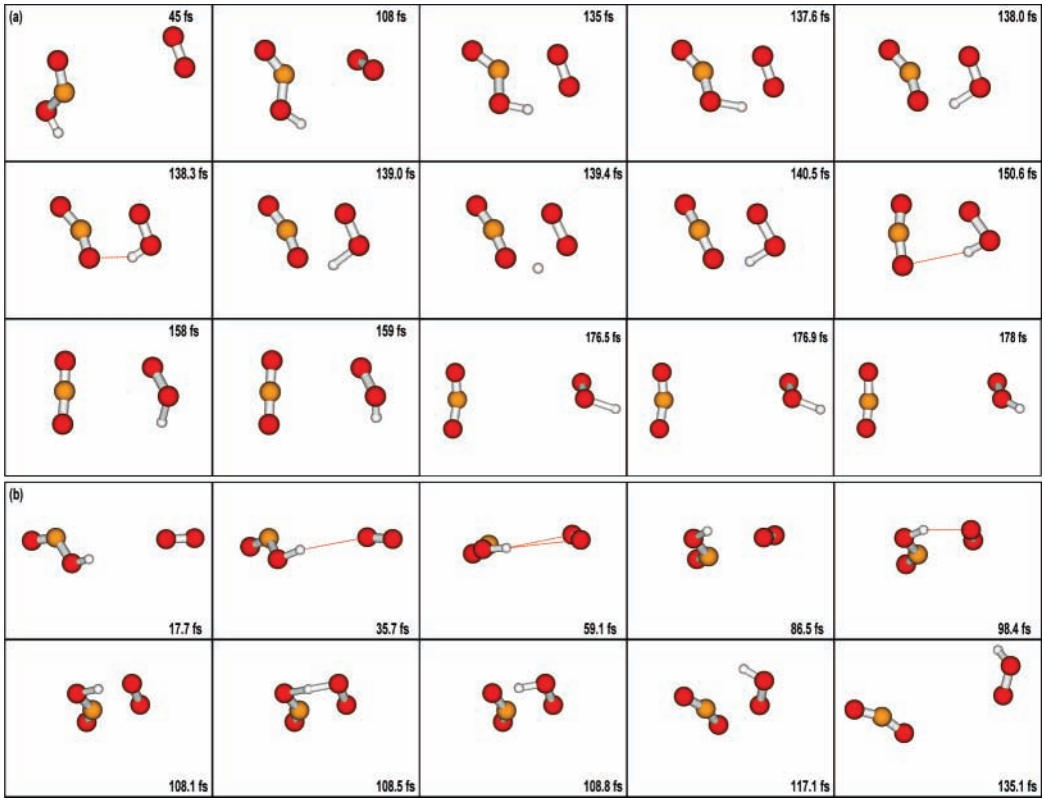

Figure 3. Two typical reactive trajectories via a direct abstraction mechanism: (a) products are vibrationally hot; (b) products are vibrationally cold. The time is indicated in each frame.

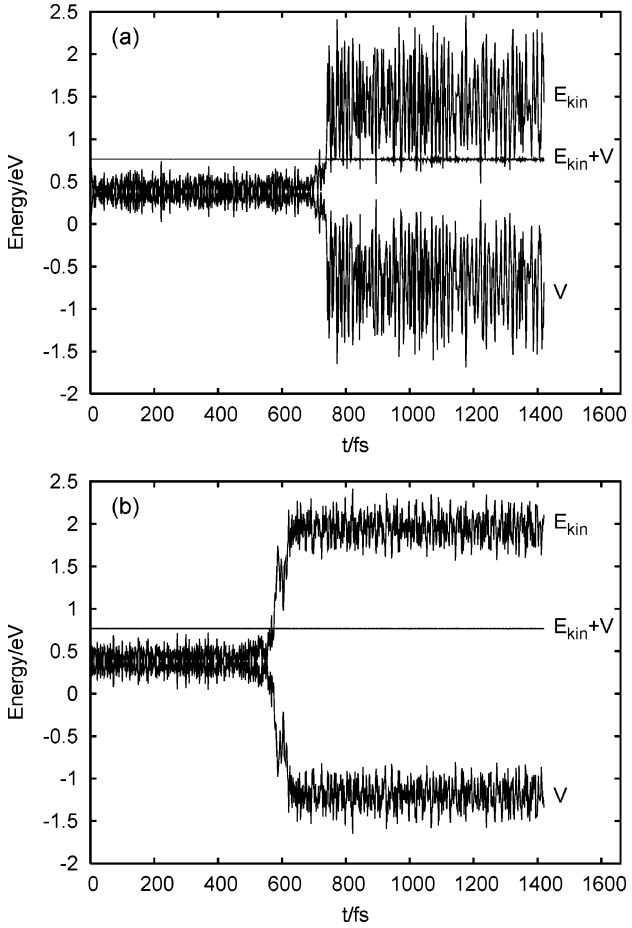

Figure 4. Energy curves for the two typical reactive trajectories via a direct abstraction pathway shown in Figure 3. The kinetic and potential energies and the total energy are indicated by the labels.

parameter, initial orientation, and vibrational phases of the reactants are different. The impact parameters are 2.7354 a_0 for trajectory (a) and 2.0683 a_0 for trajectory (b).

The snapshots in Figure 3 clearly demonstrate that the direct abstraction reaction occurs when one oxygen atom in O_2 approaches the hydrogen atom in HOCO. The hydrogen transfer is finished within 25 fs. We also noticed that this process is largely guided by hydrogen bond energy. As the collision energy increases, the hydrogen bond energy plays a lesser role. Consequently, the fraction of the direct abstraction reactions will decrease. This tendency is exactly what is observed, as shown in Table 2.

In addition, the energy disposal in products is apparently different for the two selected trajectories. Trajectory (a) has a highly vibrationally excited HO_2 molecule, whereas trajectory (b) releases most of the energy into translational motion. The snapshots from the time of 149.5 fs to 178 fs in Figure 3a show that the newly formed O−H bond vibrates strongly when the HO_2 separates from CO_2. In contrast, the separation speed of the HO_2 and CO_2 products is faster for trajectory (b) than for trajectory (a). This finding is clearly shown in Figure 4. The calculated translational energy of the products is 8.30 kcal/mol for trajectory (a) and 35.11 kcal/mol for trajectory (b), of the total energy release of 61.45 kcal/mol. The remaining energy is partitioned in the rovibrational motion of the products.

Another typical trajectory for the addition mechanism is shown in Figure 5. A short-lived $HOC(O)O_2$ complex is formed at the time of 63 fs by the formation of a new C−O bond. The resulting energized intermediate survives for about 190 fs until it reaches a TSb-like structure at the time of 255 fs. After a quick hydrogen transfer, the products are produced. Here, nearly two-thirds of the total energy disposal is released into the translational motion of the products. This is because the exit transition state (TSb) has a compact five-membered-ring structure with a small barrier height of 4.2 kcal/mol with respect to the minimum of $HOC(O)O_2$.

In a manner similar to our previous work,[54] we can calculate the lifetime of the intermediate in terms of its survival probability ($P_S(t)$) as a function of time. Figure 6 is a logarithmic plot of $P_S(t)$ for a collision energy of 2.5 kcal/mol. From the slope of the histogram, we have extracted the lifetime of the $HOC(O)O_2$ complex as $\tau = 660 \pm 30$ fs. This lifetime is shorter than the rotational period of molecule; therefore, the energy distribution and the scattering direction of the products should show a strong non-RRKM behavior. The short lifetime also implies that the $HOC(O)O_2$ intermediate is less likely to be stabilized during the O_2 + HOCO → HO_2 + CO_2 reaction at low pressure. This argument supports the assumption made by Miyoshi and co-workers[41] in their experiments but is inconsistent with the suggestion of Olkhov et al.[45] that there is a stabilized $HOC(O)O_2$ intermediate.

4. Summary

We have performed an ab initio molecular dynamics study on the O_2 + HOCO → HO_2 + CO_2 reaction, in which the forces were evaluated with a density functional theory (UB3PW91/6-31G(d)) method. The dynamics results reveal two reaction mechanisms, a direct abstraction and an addition one. The addition mechanism proceeds via a short-lived $HOC(O)O_2$ intermediate, whose lifetime is predicted to be about 660 fs. In addition, the reaction is slow at low temperatures. At room temperature, the calculated thermal rate coefficient is 2.1×10^{-12} cm^3 molecule^{-1} s^{-1}, which is in good agreement with the experimental results available. Finally, this is an activated reaction but with a small activation energy of 0.71 kcal/mol.

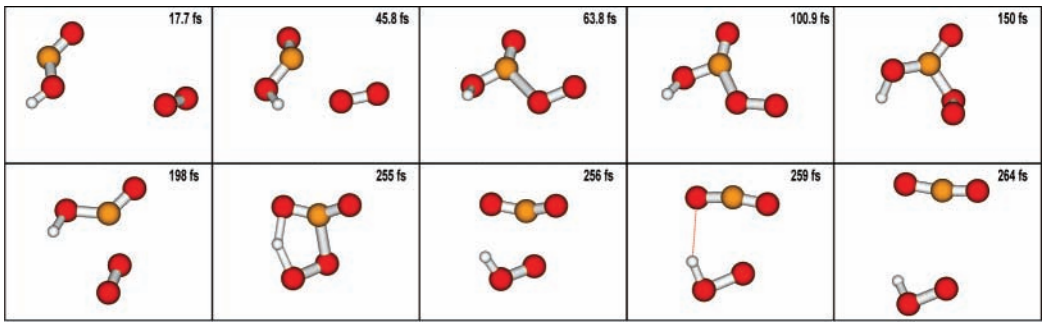

Figure 5. Reactive trajectory via a short-lived $HOC(O)O_2$ complex. The time is given in each panel.

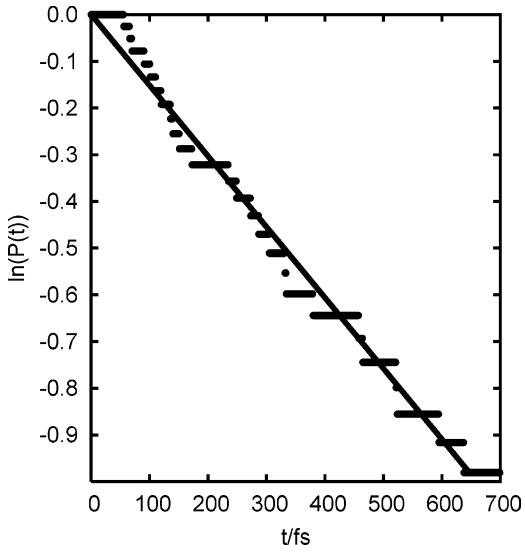

Figure 6. Logorithm of the survival probability of the intermediate $HOC(O)O_2$ as a function of time at a collision energy of 2.5 kcal/mol.

Acknowledgment. This work was performed at Brookhaven National Laboratory under contract no. DE-AC02-98CH10886 with the U. S. Department of Energy and supported by its Division of Chemical Sciences, Office of Basic Energy Sciences.

References and Notes

(1) Bowan, C. T. In *Fossil Fuel Combustion*; Wiley: New York, 1991.
(2) Wayne, R. P. *Chemistry of Atmospheres*, 2nd ed.; Clarendon: Oxford, 1991.
(3) Weston, R. E. *Chem. Rev.* **1999**, *99*, 2115.
(4) Ravishankara, A. R.; Thompson, R. L. *Chem. Phys. Lett.* **1983**, *99*, 377.
(5) Jonah, C. D.; Mulac, W. A.; Zeglinski, P. *J. Phys. A* **1984**, *88*, 4100.
(6) Golden, D. M.; Smith, G. P.; McEwen, M. C.; Yu, C.-L.; Eiteneer, B.; Frenklach, M.; Vaghjiani, G. L.; Ravishankara, A. R.; Tully, F. P. *J. Phys. Chem. A* **1998**, *102*, 8598.
(7) Alagia, M.; Balucani, N.; Casavecchia, P.; Stranges, D.; Volpi, G. G. *J. Chem. Phys.* **1993**, *98*, 8341.
(8) Forster, R.; Frost, M.; Fulle, D.; Hamann, H. F.; Hippler, H.; Schlepegrell, A.; Troe, J. *J. Chem. Phys.* **1995**, *103*, 2949.
(9) Fulle, D.; Hamann, H. F.; Hippler, H.; Troe, J. *J. Chem. Phys.* **1996**, *105*, 983.
(10) van Beek, M. C.; ter Meulen, J. J. *J. Chem. Phys.* **2001**, *115*, 1843.
(11) Pollack, I. B.; Tsiouris, M.; Leung, H. O. *J. Chem. Phys.* **2003**, *119*, 118.
(12) Pond, B. V.; Lester, M. I. *J. Chem. Phys.* **2003**, *118*, 2223.
(13) Marshall, M. D.; Pond, B. V.; Lester, M. I. *J. Chem. Phys.* **2003**, *118*, 1196.
(14) Clements, T. G.; Continetti, R. E.; Francisco, J. S. *J. Chem. Phys.* **2002**, *117*, 6478.
(15) Lester, M. I.; Pond, B. V.; Anderson, D. T.; Harding, L. B.; Wagner, A. F. *J. Chem. Phys.* **2000**, *113*, 9889.
(16) Zhu, R. S.; Diau, E. G. W.; Lin, M. C.; Mebel, A. M. *J. Phys. Chem.* **2001**, *A105*, 11249.
(17) Bradley, K. S.; Schatz, G. C. *J. Chem. Phys.* **1997**, *106*, 8464.
(18) Hernández, M. I.; Clary, D. C. *J. Chem. Phys.* **1994**, *101*, 2779.
(19) Christoffel, K. M.; Bowman, J. M. *J. Phys. Chem.* **1999**, *A103*, 3020.
(20) Clary, D. C.; Schatz, G. C. *J. Chem. Phys.* **1993**, *99*, 4578.
(21) Goldfield, E. M.; Gray, S. K.; Schatz, G. C. *J. Chem. Phys.* **1995**, *102*, 8807.
(22) Zhang, D. H.; Zhang, J. Z. H. *J. Chem. Phys.* **1995**, *103*, 6512.
(23) Feiberg, K. L.; Billing, G. D.; Johnson, M. S. *J. Phys. Chem. A* **2001**, *105*, 11171.
(24) Mozurkewich, M.; Benson, S. W. *J. Phys. Chem.* **1984**, *88*, 6429.
(25) Billing, G. D.; Muckerman, J. T.; Yu, H.-G. *J. Chem. Phys.* **2002**, *117*, 4755.
(26) Yu, H.-G.; Muckerman, J. T.; Sears, T. J. *Chem. Phys. Lett.* **2001**, *349*, 547.
(27) Yu, H.-G.; Muckerman, J. T. *J. Chem. Phys.* **2002**, *117*, 11139.
(28) Duncan, T. V.; Miller, C. E. *J. Chem. Phys.* **2000**, *113*, 5138.
(29) Francisco, J. S. *J. Chem. Phys.* **1997**, *107*, 9039.
(30) Senosiain, J. P.; Klippenstein, S. J.; Miller, J. A. *Proc. Combust. Inst.* **2005**, *30*, 945.
(31) Feilberg, K. L.; Johnson, M. S.; Nielsen, C. J. *Phys. Chem. Chem. Phys.* **2005**, *7*, 2318.
(32) Valero, R.; Kroes, G. J. *J. Phys. Chem. A* **2004**, *108*, 8672.
(33) Valero, R.; McCormack, D. A.; Kroes, G. J. *J. Chem. Phys.* **2004**, *120*, 4263.
(34) Medvedev, D. M.; Gray, S. K.; Goldfield, E. M. *J. Chem. Phys.* **2004**, *120*, 1231.
(35) Lakin, D.; Troya, M. J.; Schatz, G. C. *J. Chem. Phys.* **2003**, *119*, 5848.
(36) Senosiain, J. P.; Musgrave, C. B.; Golden, D. M. *Int. J. Chem. Kinet.* **2003**, *35*, 464.
(37) Milligan, D. E.; Jacox, M. E. *J. Chem. Phys.* **1971**, *54*, 927.
(38) Sears, T. J.; Fawzy, W. M.; Johnson, P. M. *J. Chem. Phys.* **1992**, *97*, 3996.
(39) Petty, J.; Moore, C. B. *J. Mol. Spectrosc.* **1993**, *161*, 149.
(40) DeMore, W. B. *Int. J. Chem. Kinet.* **1984**, *16*, 1187.
(41) Miyoshi, A.; Matsui, H.; Washida, N. *J. Chem. Phys.* **1994**, *100*, 3532.
(42) Paragkeropoulous, G.; Irwin, R. S. *J. Chem. Phys.* **1984**, *80*, 259.
(43) Hufzumahaus, A.; Stuhl, F. *Ber. Bunsen-Ges. Phys. Chem.* **1984**, *88*, 557.
(44) McCabe, D. C.; Gierczak, T.; Talukdar, R. K.; Ravishankara, A. R. *Geophys. Res. Lett.* **2001**, *28*, 3135.
(45) Olkhov, R. V.; Li, Q.; Osborne, M. C.; Smith, I. W. M. *Phys. Chem. Chem. Phys.* **2001**, *3*, 4522.
(46) Petty, J. T.; Harrison, J. A.; Moore, C. B. *J. Phys. Chem.* **1993**, *97*, 11194.
(47) Nolte, J.; Grussdorf, J.; Temps, F.; Wagner, H. Gg. *Z. Naturforsch., A: Phys. Sci.* **1993**, *48*, 1234.
(48) Poggi, G.; Francisco, J. S. *J. Chem. Phys.* **2004**, *120*, 5073.
(49) Yu, H.-G.; Muckerman, J. T.; Francisco, J. S. *J. Phys. Chem. A* **2005**, *109*, 5230.
(50) Yu, H.-G.; Muckerman, J. T. *J. Phys. Chem. A* **2004**, *108*, 8615.
(51) Frisch, M. J.; Trucks, G. W.; Schlegel, H. B.; Scuseria, G. E.; Robb, M. A.; Cheeseman, J. R.; Montgomery, J. A., Jr.; Vreven, T.; Kudin, K. N.; Burant, J. C.; Millam, J. M.; Iyengar, S. S.; Tomasi, J.; Barone, V.; Mennucci, B.; Cossi, M.; Scalmani, G.; Rega, N.; Petersson, G. A.; Nakatsuji, H.; Hada, M.; Ehara, M.; Toyota, K.; Fukuda, R.; Hasegawa, J.; Ishida, M.; Nakajima, T.; Honda, Y.; Kitao, O.; Nakai, H.; Klene, M.; Li, X.; Knox, J. E.; Hratchian, H. P.; Cross, J. B.; Bakken, V.; Adamo, C.; Jaramillo, J.; Gomperts, R.; Stratmann, R. E.; Yazyev, O.; Austin, A. J.; Cammi, R.; Pomelli, C.; Ochterski, J. W.; Ayala, P. Y.; Morokuma, K.; Voth, G. A.; Salvador, P.; Dannenberg, J. J.; Zakrzewski, V. G.; Dapprich, S.; Daniels, A. D.; Strain, M. C.; Farkas, O.; Malick, D. K.; Rabuck, A. D.; Raghavachari, K.; Foresman, J. B.; Ortiz, J. V.; Cui, Q.; Baboul, A. G.; Clifford, S.; Cioslowski, J.; Stefanov, B. B.; Liu, G.; Liashenko, A.; Piskorz, P.; Komaromi, I.; Martin, R. L.; Fox, D. J.; Keith, T.; Al-Laham, M. A.; Peng, C. Y.; Nanayakkara, A.; Challacombe, M.; Gill, P. M. W.; Johnson, B.; Chen, W.; Wong, M. W.; Gonzalez, C.; Pople, J. A. *Gaussian 03*, revision B.04; Gaussian, Inc.: Wallingford, CT, 2004.
(52) Faist, M. B.; Muckerman, J. T.; Schubert, F. E. *J. Chem. Phys.* **1978**, *69*, 4087.
(53) Muckerman, J. T.; Faist, M. B. *J. Phys. Chem.* **1979**, *83*, 79.
(54) Yu, H.-G.; Muckerman, J. T. *J. Phys. Chem. A* **2005**, *109*, 1890.
(55) Guo, Y.; Thompson, D. L.; Sewell, T. D. *J. Chem. Phys.* **1996**, *104*, 576.
(56) Yu, H.-G.; Varandas, A. J. C. *J. Chem. Soc., Faraday Trans.* **1997**, *93*, 2651.
(57) Scott, A. P.; Radom, L. *J. Phys. Chem.* **1996**, *100*, 16502.